Available online at www.sciencedirect.com

ScienceDirect

Procedia Structural Integrity 49 (2023) 16–22

Structural Integrity Procedia

www.elsevier.com/locate/procedia

Medical Devices: Materials, Mechanics and Manufacturing

On the validation of patient-specific numerical simulations of the TEVAR procedure

Anna Ramella[a], Francesco Migliavacca[a], Josè Felix Rodriguez Matas[a], Tim J Mandigers[b,c], Maurizio Domanin[b,d], Daniele Bissacco[b,d], Robin H. Heijmen[e], Santi Trimarchi[b,d], Giulia Luraghi[a,*]

[a] *Department of Chemistry, Materials and Chemical Engineering, Politecnico di Milano, Piazza L. da Vinci 32, 20133 Milan, Italy*
[b] *Unit of Vascular Surgery, I.R.C.C.S. Fondazione Ca' Granda Policlinico Milano, Via Francesco Sforza 35, Milan, Italy*
[c] *Department of Vascular Surgery, University Medical Center Utrecht, Heidelberglaan 100 3584 CX Utrecht, The Netherlands*
[d] *Clinical and Community Sciences Department, Universita` degli Studi di Milano, Via della Commenda 19, 20122 Milan, Italy*
[e] *Department of Cardiothoracic Surgery, Radboud University Medical Center, Geert Grooteplein Zuid 10, 6525 GA Nijmegen*

Abstract

The Thoracic Endovascular Aortic Repair (TEVAR) is becoming the first choice to treat thoracic aortic pathologies (e.g., aneurysms, ulcerations, and dissections) in a minimally invasive way. It consists of placing a self-expandable stent-graft into the pathological region to recreate a more physiological condition. When computational models are used in this clinical context to predict procedural results, their credibility should be validated and verified. This works applies a validated finite element methodology to four patient-specific anatomies. Different sizes of a commercial stent-graft model are recreated, and the TEVAR simulation results are validated by comparing them to post-operative Computed Tomography images. Errors between simulation and segmentation are lower than 10% for the stent struts opening area. This study also evaluates and discusses numerical quantities (contact pressures, device-to-vessel distances, and stress distributions) associated with potential TEVAR complications such as device migration and bird beak phenomenon. This work aims at demonstrating how a fully validated methodology is useful for clinicians to identify the best treatment for the patient before the intervention to avoid device-related complications.

* Corresponding author. Tel.: +39 02 2399 3399.
E-mail address: giulia.luraghi@polimi.it

2452-3216
10.1016/j.prostr.2023.10.004

Keywords: Stent-graft, Finite Element, Thoracic Endovascular Aortic Repair, V&V

1. Introduction

Since the first Food and Drug Administration (FDA) stent-graft approval, the minimally invasive Thoracic Endovascular Aortic Repair (TEVAR) technique has been increasingly used to treat thoracic aortic pathologies, such as aneurysms, ulcerations or dissections. It consists of placing a self-expandable stent-graft into the pathological region through a catheter inserted from the femoral artery. Stent-grafts are composed of a PET or ePTFE fabric graft sutured to a metallic nitinol stent, which accounts for structural support to both the graft and the aortic wall (Nation and Wang (2015)). TEVAR has shown a high 30-day survival rate with respect to open repair; however, despite being a low-risk treatment, procedure-related complications in the long term still remain unclear. Most complications (e.g., endoleaks, migration, compliance mismatch) are generally associated with a suboptimal apposition of the stent-graft to the aortic wall. Therefore, the procedural success of TEVAR has strictly related to appropriate patient/stent-graft selection and stent-graft/aorta mechanical interaction (Daye and Walker (2018)).

In recent years, the computational biomechanics community has shown great interest in the development of patient-specific in silico models to investigate the TEVAR procedure from an engineering point of view and to assess quantitative parameters to better understand device performances. In this context, when employing numerical models for clinical applications, it is crucial to establish their reliability and credibility, as recommended by the V&V40 standard set by the American Society of Mechanical Engineering (American Society of Mechanical Engineers (2018)). To address this, some studies (Kan et al. (2021); Perrin et al. (2015); Romarowski et al. (2019)) have conducted TEVAR model validation by comparing simulation results with stent segmented from patient-specific Computed Tomography (CT) images. Their validation process involved both qualitative and quantitative analyses, including the calculation of the opening radius/diameter of the simulated and segmented stent struts at the end of the deployment phase.

Within this context, the purpose of this work is to apply a recently validated high-fidelity finite element (FE) methodology (Ramella et al. (2022)) to virtually reproduce the TEVAR procedure in four patient-specific anatomies. In particular, the process of aortic anatomies segmentation from clinical images, the stent-graft modeling, and the numerical deployment simulation are described. The pre-stress field in the aortic wall is also included. Simulation outcomes are validated with post-operative CT image reconstructions, and the results are discussed by analyzing numerical quantities related to the most common complications.

2. Methods

2.1. Patient-specific data

The study included four patients who underwent TEVAR. Two anatomies were provided by the Fondazione IRCCS Ca' Granda Ospedale Maggiore Policlinico in Milan, Italy (patients 1 and 2), while the other two were provided by the St. Antonius Hospital, Nieuwegein, The Netherlands (patients 3 and 4). Details regarding the patients' pathologies, stent-graft landing zones (Marrocco-Trischitta et al. (2018)), and device sizes are listed in Table 1. Follow-up CT scans conducted two months after the surgery confirmed the accurate placement of the thoracic aortic endografts without complications. The study included four anonymized patients' CTs who underwent TEVAR. Approval for this specific study was waived by the local ethical committees.

2.2. Numerical simulation set-up

FE models of Valiant Captivia stent-grafts were recreated starting from the work by Ramella et al. (2022): the stent and the graft were respectively discretized with beam elements (average size of 1 mm) and triangular membrane elements (average size of 1 mm) (Tab. 2). The nitinol material (for the stent) was modeled using a shape memory material formulation, while a fabric material with no resistance to compression was assigned to the PET (for the graft). Material parameter details can be found in Ramella et al. (2022).

Table 1. Information about the four patients included in the study (abbreviations: diam = diameter)

Patient ID	Pathology	Stent-graft landing zone	Stent-graft size (proximal diam x distal diam x length) [mm]
1	PAU	Zone 2	34 x 34 x 100
2	PAU + intraluminal thrombus	Zone 2	32 x 32 x 100
3	PAU	Zone 2	38 x 38 x 100
4	IMH	Zone 3	36 x 36 x 200

Pre-operative aortic models were segmented from CT images using the VMTK (Orobix srl, Italy) software. The segmented anatomies comprised the ascending aorta, aortic arch, descending aorta, supraortic vessels and the pathological region (Fig. 1). Solid meshes were created in the same way for all the anatomies: the segmented surface models were discretized with triangular elements then extruded to generate three layers of tetrahedrons (average size of 0.6 mm). The thickness was assigned following the values reported in the literature (Choudhury et al. (2009)) since it was not possible to derive it from CT scans: it varied from 1.8 mm (ascending, descending aorta and aortic arch) to 1 mm (supraortic branches). The vessel material was modeled with an isotropic hyperelastic law following the second-order Yeoh constitutive formulation with literature material parameters. Patient 2 presented an intraluminal thrombus modelled with the same material model of the vessel but softer (Simsek and Kwon (2015)). The vessel pre-stress due to blood pressure was included following an inverse elastostatic method implemented within the ANSYS Mechanical FEA software (Ansys Inc., Canonsburg, PA, USA) (Govindjee and Mihalic (1996)).

Simulations to replicate the TEVAR procedure followed the steps reported in our previous studies (Ramella et al. (2023, 2022)). The device was initially crimped and displaced along the vessel centerline until the proximal landing zone was reached; then, it was gradually released from a proximal towards a distal region. Fig.1 depicts the steps of the simulation for each anatomy.

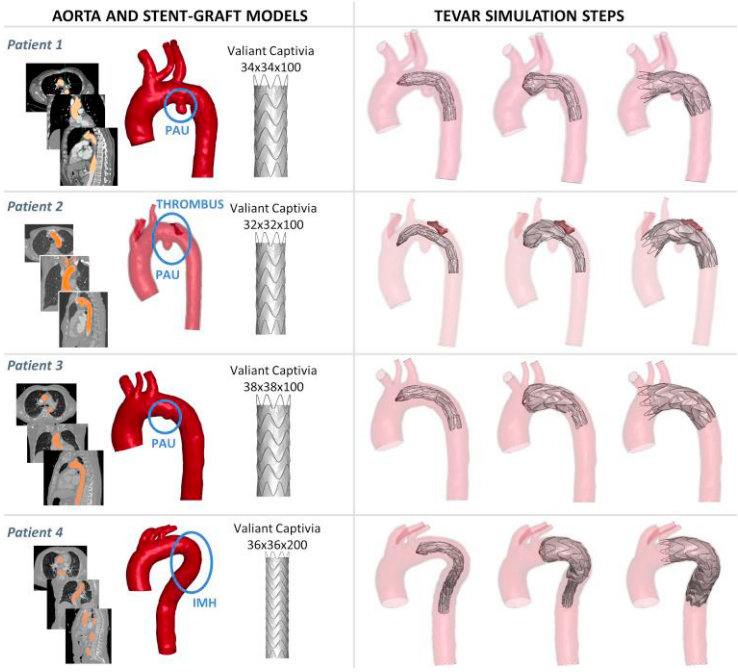

Fig. 1: On the left, anatomies reconstruction from CT images and stent-graft model for each patient. On the right, three steps of the TEVAR simulation for each patient.

To validate patient-specific simulations, the stent deployed configurations obtained with numerical simulations were compared with the stents segmented from post-operative CT images. This comparison included a qualitative overlap of the two configurations and a quantitative analysis of the opening area (OA) percentage error for each single stent ring, as discussed in Ramella et al. (2022). The OA was defined as the area enclosed by the spline fitted into the apexes of each stent ring, while the error was calculated as the difference between the segmentation OA and simulation OA over the segmentation OA.

Furthermore, the simulation results were examined in terms of normal contact pressures on the vessel wall, distances between the stent and the vessel, and von Mises stresses in the aorta. These quantities were investigated as they can be associated with potential TEVAR complications (Hemmler et al. (2019)).

Finite element (FE) simulations were performed on 28 CPUs of an Intel Xeon64 with 250 GB of RAM using the commercial explicit finite element solver LS-DYNA 971 Release 14.1 (ANSYS, Canonsburg, PA, USA). All the FE grids were created using ANSA Pre Processor v23.0.1 (BETA CAE Systems, Switzerland) and the post-processing analysis was done with META Post Processor v22.0 (BETA CAE System, Switzerland).

3. Results and discussions

3.1. Simulation validation

Figure 2 depicts the comparison between the simulation and the post-operative CT segmentation. A good qualitative overlap between the segmented and simulated stent configurations was achieved for every patient. Then, by evaluating the OA at each stent strut, OA percentage errors between the simulation and CT reconstruction were always found to be below 10%, lower if compared to other literature studies (Kan et al. (2021); Perrin et al. (2015); Romarowski et al. (2019)). Error values were higher for patients 1 and 2 at the level of the pathology. In particular, for patient 2, differences were located at the struts in contact with the thrombus (stent strut number 5). In all the anatomies, low errors (below 5%) were registered in the proximal ring, which plays a crucial role in guaranteeing the anchoring of the device to the aortic wall.

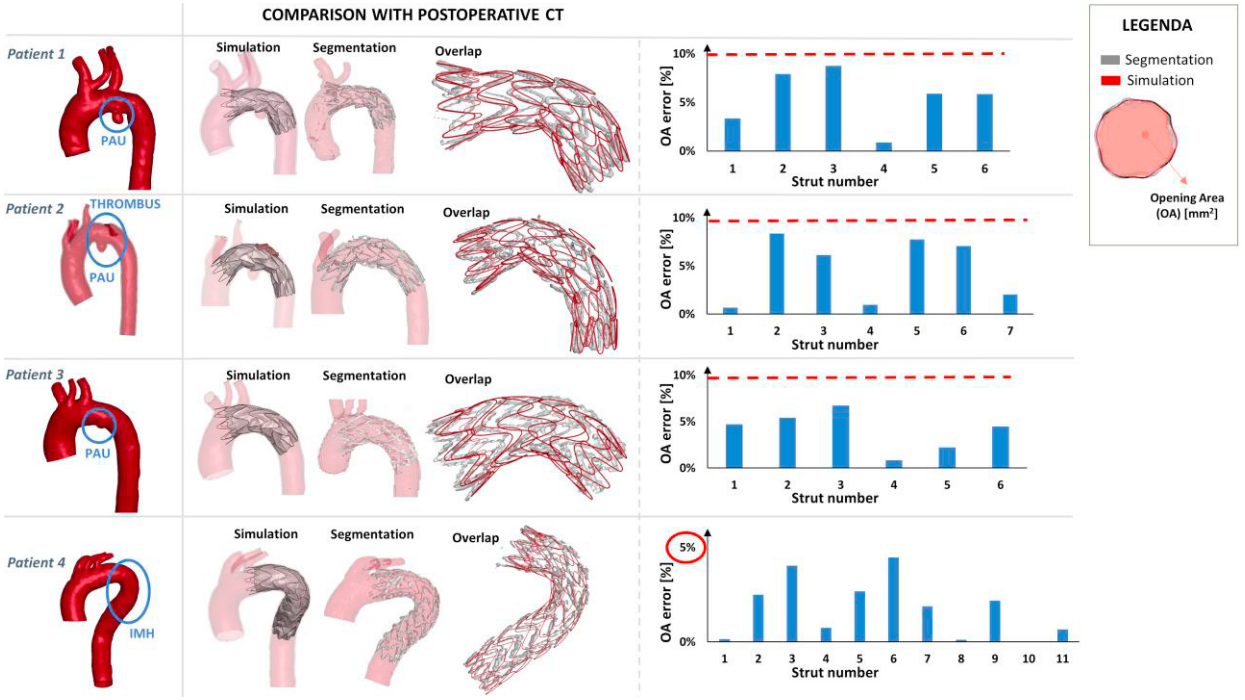

Fig.2: Qualitative validation of the simulation by comparing the numerical results (red) with the stent reconstructed from CTA images (grey). On the right the quantification of the opening area (OA) error for each stent strut.

3.2. Simulation results and TEVAR complications

Normal contact pressures and device-to-vessel distances were assessed to determine the outcome of the simulated surgical procedure. They served as indicators of the quality of the device apposition to the aortic wall and the interactions between the stent and the vessel. Moreover, these parameters also have implications for the occurrence of the bird-beak phenomenon and device migration (Hemmler et al. (2019); Shahbazian et al. (2022)). The bird beak phenomenon is characterized by a gap between the aorta wall and the stent-graft with a stent protrusion in the lumen of greater than 5 mm. It results from an improper apposition at the proximal end of the thoracic endograft caused by a lesser curve of the proximal landing zone (Daye and Walker (2018)).

The contact pressure analysis (Fig.3-a) revealed an overall maximum value of 23.7 kPa (with specific maximum values of 26.1 kPa, 24.2 kPa, 21.2 kPa and 24.7 kPa for patients 1, 2, 3, and 4, respectively). Globally, high values were located in the regions of the vessel in contact with the stent. The contact pressure was strictly related to the amount of stent-graft oversizing (indicated by the manufacturer's Instruction for Use (IFU) manual) with respect to the aortic diameter in the landing zone. In all simulated cases, the device oversizing adhered to the IFU guidelines, which explains the similarity in maximum pressure values among the patients. However, patient-specific local variations can be due to differences in the aortic shape (i.e., curvature, tortuosity) and landing zones.

Similar considerations can be derived regarding the distances between the device and the aorta (Fig.3-b). The majority of the stent struts were attached to the aortic wall (distance 0 mm), while greater distance values were found in the graft regions due to foldings (indicated as example by the red arrow in Fig.3-b). In the proximal part of the first ring, distances increased (> 1.5 mm) because there was a loss in contact due to the aortic curvature (i.e., development of possible bird beak phenomenon). However, in all the patients, the sealing was ensured in the proximal graft region (region highlighted by the red box in Fig.3-b).

Additionally, the study examined the aortic stresses that were generated after the implantation of the device as indicators of possible vascular damage following the procedure (Fig.3-c). The peak stress values were located at the origin of the supraortic branches or on the external curvature of the vessel and, however, can be attributed to the inclusion of vessel pre-stress. In patient 4, these peak stress values reached a maximum of 2.1 MPa. It is important to state that in all the studied anatomies, the stent-graft implantation resulted in increased stress values in the aortic wall.

4. Conclusions

Ensuring the reliability and accuracy of numerical models is of utmost importance when models are employed to study clinical procedures. The high-fidelity methodology proposed in this work has been recently verified and validated using a rigid idealized aortic model (Ramella et al. (2022)) and its applicability to patient-specific scenarios was demonstrated as well (Ramella et al. (2023)).

In the present work, four patient-specific anatomies were involved to accurately replicate and validate the thoracic endovascular aortic repair (TEVAR) procedure in realistic scenarios. Post-operative CT images and indications by clinicians were employed to reconstruct and implant different stent-graft models in the same landing zone as in the actual clinical scenarios. The comparison of the simulation results with post-operative CT image segmentation allows us to validate the model in a realistic framework and has demonstrated the capability of our numerical tool to faithfully replicate the TEVAR procedure in patient-specific aortas given a validated stent-graft model. Moreover, the analyzed numerical parameters (contact pressures, device-to-aorta distances, von Mises stress distributions in the aorta) highlighted the potentiality of the method to investigate common device-related procedural complications such as device migration, bird beak presence or damages to the aortic wall.

This study might open up new possibilities for clinicians to utilize a numerical methodology during the procedural planning phase. It might enable them to determine the optimal landing zone, particularly in complex arch anatomies cases or more distal descending aortic angulation and tortuosity. Furthermore, the methodology can be expanded to include other commercially available devices. This enables the investigation of the TEVAR procedure outcomes with different stent-graft models and sizes in patient-specific anatomies. By utilizing this approach, it becomes possible to find the most suitable treatment option for each patient prior to the intervention.

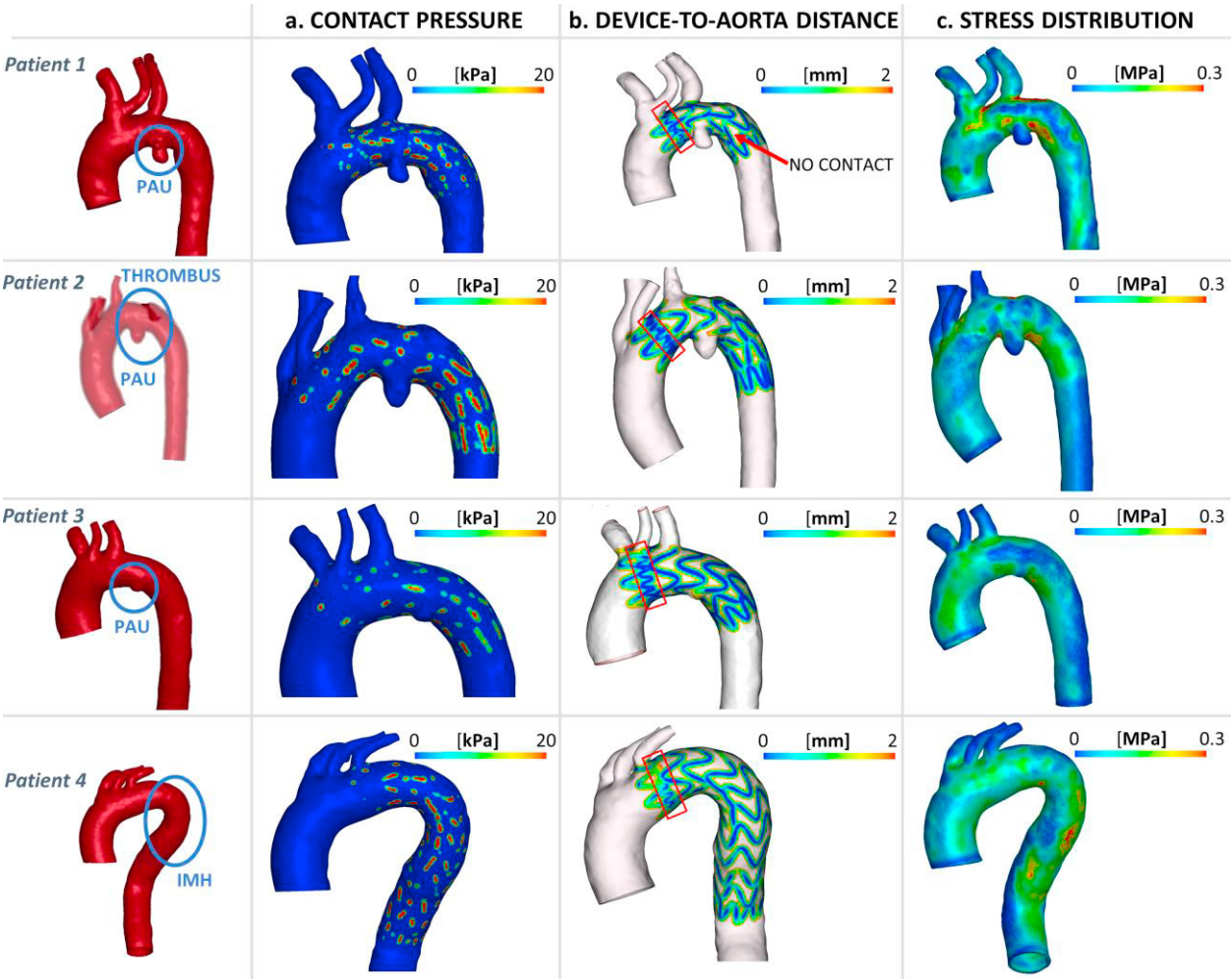

Fig. 3: Numerical parameters at the end of the TEVAR simulation: (a.) contact pressure (kPa), (b.) distances between the device and the aorta (mm), and (c.) von Mises stress distribution on the aorta (MPa). In the distance column, the red arrow indicates an example of a non-contact region, while the red rectangle highlights the proximal graft rim.

Acknowledgements

This study has received funding from the MIUR FISR-FISR2019_03221 CECOMES. FM is partially supported by the MUSA – Multilayered Urban Sustainability Action – project, funded by the European Union – NextGenerationEU, under the National Recovery and Resilience Plan (NRRP) Mission 4 Component 2 Investment Line 1.5: Strengthening of research structures and creation of R&D "innovation ecosystems", set up of "territorial leaders in R&D".

References

American Society of Mechanical Engineers, 2018. Assessing credibility of computational modeling through verification and validation: application to medical devices - V&V40-2018. Asme V&V 40-2018.

Choudhury, N., Bouchot, O., Rouleau, L., Tremblay, D., Cartier, R., Butany, J., Mongrain, R., Leask, R.L., 2009. Local mechanical and structural

properties of healthy and diseased human ascending aorta tissue. Cardiovasc. Pathol. 18, 83–91. https://doi.org/10.1016/J.CARPATH.2008.01.001

Daye, D., Walker, T.G., 2018. Complications of endovascular aneurysm repair of the thoracic and abdominal aorta: evaluation and management. Cardiovasc. Diagn. Ther. 8, S138. https://doi.org/10.21037/CDT.2017.09.17

Govindjee, S., Mihalic, P.A., 1996. Computational methods for inverse finite elastostatics. Comput. Methods Appl. Mech. Eng. 136, 47–57. https://doi.org/10.1016/0045-7825(96)01045-6

Hemmler, A., Lutz, B., Reeps, C., Gee, M.W., 2019. In silico study of vessel and stent-graft parameters on the potential success of endovascular aneurysm repair. Int. j. numer. method. biomed. eng. 35. https://doi.org/10.1002/CNM.3237

Kan, X., Ma, T., Lin, J., Wang, L., Dong, Z., Xu, X.Y., 2021. Patient-specific simulation of stent-graft deployment in type B aortic dissection: model development and validation. Biomech. Model. Mechanobiol. 20, 2247–2258. https://doi.org/10.1007/S10237-021-01504-X/TABLES/4

Marrocco-Trischitta, M.M., van Bakel, T.M., Romarowski, R.M., de Beaufort, H.W., Conti, M., van Herwaarden, J.A., Moll, F.L., Auricchio, F., Trimarchi, S., 2018. The Modified Arch Landing Areas Nomenclature (MALAN) Improves Prediction of Stent Graft Displacement Forces: Proof of Concept by Computational Fluid Dynamics Modelling. Eur. J. Vasc. Endovasc. Surg. 55, 584–592. https://doi.org/10.1016/j.ejvs.2017.12.019

Nation, D.A., Wang, G.J., 2015. TEVAR: Endovascular Repair of the Thoracic Aorta. Semin. Intervent. Radiol. 32, 265–271. https://doi.org/10.1055/S-0035-1558824/ID/JR00904A-38

Perrin, D., Badel, P., Orgéas, L., Geindreau, C., Dumenil, A., Albertini, J.N., Avril, S., 2015. Patient-specific numerical simulation of stent-graft deployment: Validation on three clinical cases. J. Biomech. 48, 1868–1875. https://doi.org/10.1016/J.JBIOMECH.2015.04.031

Ramella, A., Migliavacca, F., Felix, J., Matas, R., Heim, F., Dedola, F., Marconi, S., Conti, M., Allievi, S., Mandigers, T.J., Bissacco, D., Domanin, M., Trimarchi, S., Luraghi, G., 2022. Validation and Verification of High-Fidelity Simulations of Thoracic Stent-Graft Implantation. Ann. Biomed. Eng. 2022 1–13. https://doi.org/10.1007/S10439-022-03014-Y

Ramella, A., Migliavacca, F., Felix, J., Matas, R., Mandigers, T.J., Bissacco, D., Domanin, M., Trimarchi, S., Luraghi, G., 2023. Applicability assessment for in-silico patient-specific TEVAR procedures. J. Biomech. 146, 111423. https://doi.org/10.1016/j.jbiomech.2022.111423

Romarowski, R.M., Faggiano, E., Conti, M., Reali, A., Morganti, S., Auricchio, F., 2019. A novel computational framework to predict patient-specific hemodynamics after TEVAR: Integration of structural and fluid-dynamics analysis by image elaboration. Comput. Fluids 179, 806–819. https://doi.org/10.1016/J.COMPFLUID.2018.06.002

Shahbazian, N., Doyle, M.G., Forbes, T.L., Amon, C.H., 2022. A modeling framework for computational simulations of thoracic endovascular aortic repair. Int. j. numer. method. biomed. eng. e3578. https://doi.org/10.1002/CNM.3578

Simsek, F.G., Kwon, Y.W., 2015. Investigation of material modeling in fluid-structure interaction analysis of an idealized three-layered abdominal aorta: aneurysm initiation and fully developed aneurysms. J. Biol. Phys. 41, 173–201. https://doi.org/10.1007/S10867-014-9372-X